



CHALMERS
UNIVERSITY OF TECHNOLOGY

Novel Orthomode Transducer Scalable to Terahertz Frequencies

Downloaded from: <https://research.chalmers.se>, 2026-04-15 01:17 UTC

Citation for the original published paper (version of record):

Patriksson, N., Meledin, D., Lapkin, I. et al (2024). Novel Orthomode Transducer Scalable to Terahertz Frequencies. 2024 4th URSI Atlantic Radio Science Meeting, AT-RASC 2024.
<http://dx.doi.org/10.46620/URSIATRASC24/IPKB8830>

N.B. When citing this work, cite the original published paper.



Novel Orthomode Transducer Scalable to Terahertz Frequencies

Nils Patriksson, Denis Meledin, Igor Lapkin, Cristian López, Alexey Pavolotsky, Leif Helldner, Sven Erik Ferm, Vincent Desmaris and Victor Belitsky
Group for Advanced Receiver Development, Department of Space, Earth and Environmental Sciences,
Chalmers University of Technology, Gothenburg, SE-41296, Sweden

Abstract

We present the design of a novel orthomode transducer, OMT, suitable for scaling up to Terahertz frequencies. The current design aims for the frequency band 270-380 GHz. The OMT combines waveguide components made with conventional milling with substrate-based parts fabricated using microfabrication techniques. This allows critical dimensions of the OMT conventionally to be mechanically machined parts being replaced by photolithographically defined and microfabricated structures. The paper provides details on the OMT layout, simulations, fabrication and tests. The two fabricated and tested prototype OMTs show similar performance providing better than 30 dB cross-pol suppression. The OMTs also demonstrated broadband performance with an operational band of 260-385 GHz corresponding to a 38,8% fractional bandwidth. With the microfabricated polarization splitting junction and relatively simple waveguide circuitry, the OMT has very good potential to be scaled up to higher frequencies, probably up to 1.5 THz.

1. Introduction

An orthomode transducer, OMT, is a polarization diplexer that allows to separate the polarization components of the incoming signal. A typical place for such diplexer is between the feed, e.g., a corrugated horn, and the first stage of the receiver, e.g., a mixer. Consequently, the input port of an OMT should allow the propagation of both polarizations yielding the requirement to use either square or circular waveguides, the latter is advantageously compatible with the geometry of the corrugated horn output port, while the single-mode rectangular waveguides employed as outputs for each polarization. An advantage of using OMT in a receiver system is the possibility to use a single feed for both polarizations. The shared feed employed by an OMT system for both polarizations facilitates the co-alignment of the beams for two polarizations. With a grid as polarization splitter, however, it is necessary using two separate feeds making the system bulkier, complex and more expensive.

In an OMT, the separating signals of two orthogonal polarizations should be done by structures that are placed into the input waveguide and that introduce a discontinuity for both polarizations and thus affect the modal EM field distribution. Symmetrical structures in the polarization

splitter part, e.g. when the signal of the same polarization is divided into two 180-degree shifted parts, have the advantage of generating anti-symmetric modes for another polarization [1]. By re-combining the divided by 50/50 polarization signals the unwanted antisymmetric modes are cancelled. Such principle was realized in the turnstile OMT [2] using pure waveguide structures and in planar OMTs [3] that employ a thin substrate with four E-probes. Beside the advantages of cancelling unwanted modes and being inherently very broadband, such 4-side symmetric OMTs also face the challenge to recombine each of the divided polarization signals. This requires a complex waveguide circuitry for the turnstile OMT [4] and the necessity to use complex and longer circuitry with cross-overs for planar designs [5]. The necessity of the recombining circuitry for each polarization adds to the insertion loss and largely complicates the design and fabrication of such OMTs. In our suggested OMT, we attempt to take use of both approaches, however combining the layout in a way to avoid the complexity and a higher insertion loss.

2. OMT Layout & Simulations

The suggested OMT, similarly to [3], employs E-probes fabricated on a 5 μm thin GaN substrate. In contrast to the design presented in [3], we do not use planar lines on the thin substrate for recombining the signals for each polarization but inject all 4 signals into rectangular waveguides and recombine each polarization using waveguide Y-junctions. In this way, we avoid complexity of the layout, minimize the length of the waveguides and transmission lines needed for recombining the signals of each polarization and largely reduce the challenges associated with its mechanical fabrication.

The microfabricated part, the thin substrate of the suggested OMT, is processed using photolithography providing ultimate accuracy to pattern the E-probes of the polarizations splitting junction, PSJ, transmission lines and E-probes for coupling to the rectangular waveguides. The layout of the OMT is presented in Fig. 1. The use of microfabrication for the production of the key OMT part allows potentially to scale the entire OMT to even higher frequencies.

At the first stage of the design, each part of the OMT, the PSJ with its probes, the E-probes coupled to the waveguides and the interconnecting transmission lines

were carefully optimized using Ansys HFSS™ 3D simulation software using realistic material parameters in order to reach desirable bandwidth, 270-375 GHz. Thereafter, the complete OMT was put through the final optimization.

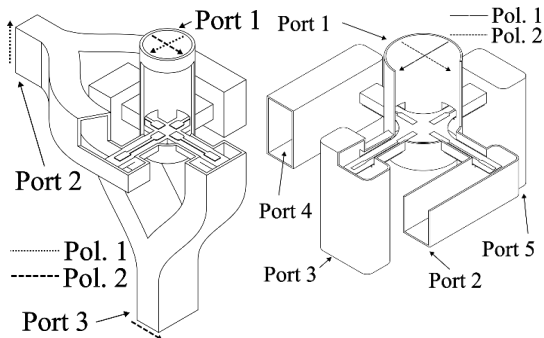


Figure 1. The OMT concept. *Left:* The full OMT model with the input circular waveguide, the polarization splitting junction, PSJ, and Y-junctions of rectangular waveguides. The microfabricated thin substrate has 4 probes of PSJ, suspended strip-lines connect PSL and E-probes coupled to rectangular waveguides for recombining each polarization. *Right:* the OMT model of the full PSJ adjusted for CNC milling with some corners rounded.

For the thin substrate, GaN was chosen based on the processing considerations and lower dielectric permittivity while the shape to be micromachined to form it optimally and leave minimum unnecessary dielectric in the PSJ and the connecting suspended strip lines to E-probes in the waveguides of the recombining circuitry. This minimalistic volume of dielectric facilitates avoiding substrate modes. The initial simulations were based on the published data [6,7] on the GaN dielectric permittivity $\epsilon_r=5.9$ for the targeted frequency band 270-380 GHz. Consequently, $\epsilon_r=7$ has been chosen as a starting value. The simulations and the OMT design tolerance analysis have shown high sensitivity of the OMT performance to the GaN dielectric permittivity. To ensure the actual value for the ϵ_r used for simulations, we performed experimental verification of the dielectric permittivity ϵ_r for the used GaN thin substrate. To obtain an actual dielectric permittivity, ϵ_r , and dielectric loss, $\tan \delta$, we fabricated a test structure consisting of the tiny GaN thin substrate with patterned split ring resonator, SRR [7, 8]. The test structure was mounted in a waveguide split block and the transmission-reflection responses were measured at actual frequencies. In the HFSS modelling, all three parameters ϵ_r , $\tan \delta$, and σ_{gold} affect the resonance frequency and the amplitude of the resonance or Q-factor but in a different manner. While changes of the GaN substrate dielectric permittivity ϵ_r mostly affect the frequency of the resonance, the varying of other two parameters produce very slight resonance frequency shift but mainly affect the Q-factor. As a result, the model fitting produced two sets of best-fit material conductivity σ_{gold} vs. dielectric loss in the GaN substrate $\tan \delta$ and the substrate dielectric permittivity closer to $\epsilon_r=8$, the value taken in the further OMT design simulation and optimization steps.

3. OMT Fabrication & Assembling

The OMT fabrication falls into two but very different steps: mechanical CNC milling for the waveguide blocks and microfabrication for the PSJ substrate. The mechanical parts were manufactured in-house using precision CNC milling machine Kern EVO. Fig. 2 shows the OMT mechanical layout that is taking use of the split-block technique. Adjusting the OMT design to the CNC milling, see some of the corners were rounded to address specific access with particular milling tools, e.g., the smallest used end mill diameter was 150 μm .

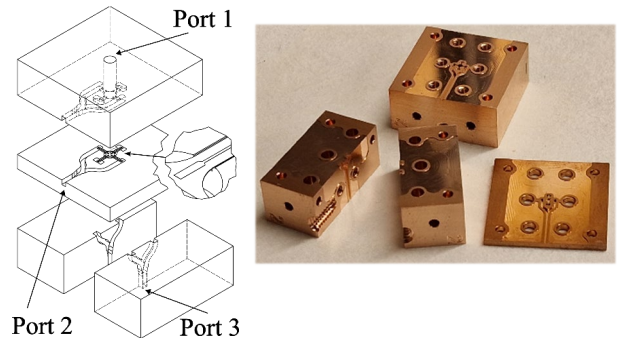


Figure 2. Mechanical model (left) and the fabricated OMT photo (right). The surface at the waveguide splits is recessed to improve the parts' joint. Port 1 is the OMT input while the outputs for two polarizations are ports 2 and 3.

The substrate part of the PSJ was manufactured using MyFab Chalmers cleanroom facility. The device fabrication was done on a 1000 μm thick Si substrate carrier with a grown buffer-layer of 3 μm AlGaIn and 2.5 μm GaN layer with total substrate size of 1x1 inch². The metallization was patterned using lift-off of the evaporated 10 nm thick Titanium adhesion layer followed by 500 nm thick Gold layer. Three different versions of the PSJ thin substrate was considered, Fig. 3, all compatible with the fabricated mechanical block. The PSJ thin substrate shaping was achieved by reactive ion etching of the GaN/AlGaIn layer followed by etching away the Silicon carrier wafer.

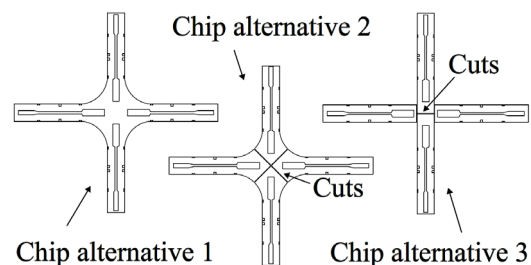


Figure 3. Versions of the PSJ thin substrate, all are compatible with the fabricated mechanical block. Alternative chip layout 2 and 3 consists of 4 separate chips. The chip layout 3 has further reduced size of the dielectric substrate placed in the input circular waveguide.

The deposited Gold films DC conductivity (σ_{gold}) was also measured using test structures with a method similar as in

[9]. Before the back-side Si etching process, σ_{gold} was measured to be 4.8×10^7 S/m and 5.25×10^7 S/m for two different test structures. After the etching process, the measured conductivity, σ_{gold} , became substantially lower, 0.82×10^7 S/m and 1.1×10^7 S/m respectively. Furthermore, the DC conductivity of GaN itself was measured after all processing steps using test structures similar to the ones for the Gold conductivity measurements. Measured conductivity, σ_{GaN} , was about 4×10^{-3} S/m and 1.5×10^{-3} S/m for the two fabricated test structures.

The assembling of the OMT with the cross PSJ substrate has faced unexpected problem. The stress gradient released in the GaN thin substrate after removing the Silicon carrier caused the substrate substantial bending and made it impossible to complete the integration of the OMT with the cross-shaped PSJ thin substrate. Thereafter, for the final OMT integration, we used the thin substrate layout depicted in Fig. 3 as “Alternative 2” and “Alternative 3”. Even though the stress gradient was present in each thin substrate, the twice shorter length made the bending acceptable and allowed us successfully and accurately place all 4 thin substrate pieces of “Alternative 2” layout into the OMT block, Fig. 4. Similarly, the assembling of “Alternative 3” layout produced another version of the OMT. The substrates were fixed at their positions by wax.

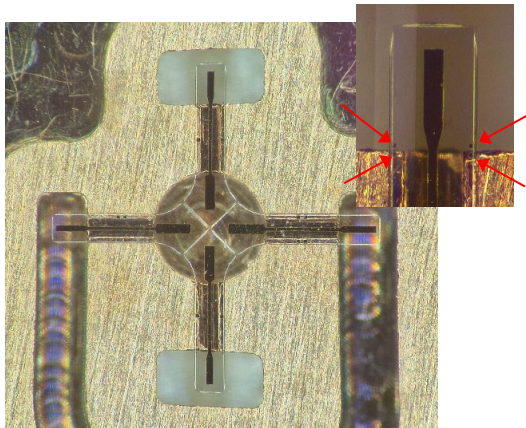


Figure 4. The microscope picture of the OMT with the PSJ thin substrate assembled from 4 separate chips, layout “Alternative 2”. The insert shows details of the alignment marks, pointed by red arrows, that allow positioning of the thin substrate with the reference to the waveguide edge.

4. OMT Testing & Discussion

The OMT was designed with non-standard rectangular waveguide dimensions of $380 \times 760 \mu\text{m}$ and $850 \mu\text{m}$ diameter of the circular input waveguide in order to cover the frequency band of interest 270-380 GHz. All OMT waveguide interfaces follow standard flange layout UG-387/U. The RF characterization of the OMT was performed at room temperature using Keysight N5242B PNA-X VNA with frequency extension modules, WR3.4 covering 220-330 GHz and WR2.2 covering 330-500 GHz. The mismatch of the waveguide dimensions was resolved by fabrication of respective adapters ensuring the compatibility of the OMT interfaces with the VNA

frequency extension modules. For the OMT’s circular waveguide port, a rectangular-to-circular waveguide adapter was fabricated to perform the measurements. A horn antenna together with a free-space absorber plate [11] was used to provide matched load simultaneously for both polarizations during the measurements, e.g. isolation between the Ports 2 and 3, as in Fig.3 left. The OMT cross-pol measurements were performed following the procedure suggested in [12]. The measurement results are presented below in Figures 5 – 7.

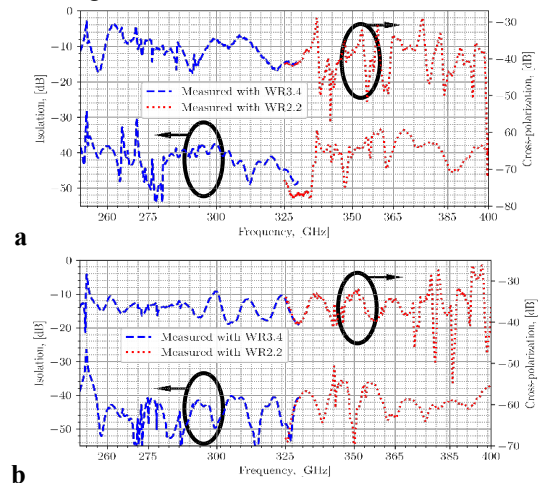


Figure 5. The isolation measurement results, lower curve, and cross-pol, upper curve. Fig. 6a with the PSJ layout, Alternative 2, and Fig. 6b for the OMT with the PSJ layout, Alternative 3.

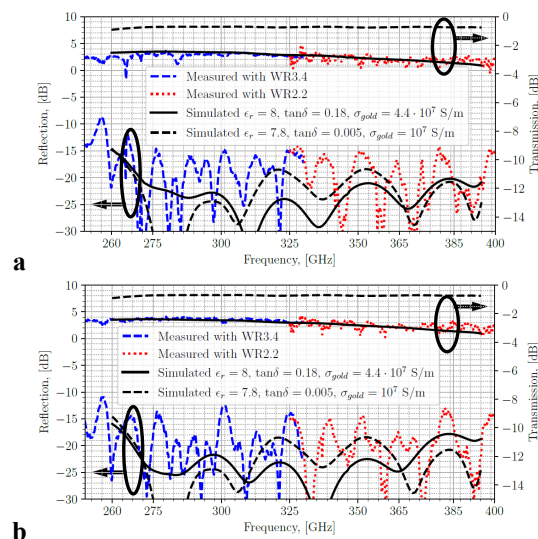


Figure 6. Measured S_{11} and S_{12} for polarization 1 & 2 in the OMT with chip Alternative 2 mounted. The measurements data in comparison with the simulations for two sets of material parameters.

The results of the measurements for the OMT with the chip Alternative 3 is very similar except for the insertion loss that are about 0.3 dB less than that of the OMT with the chip Alternative 2. From simulations and comparison with the measurements, it appears that the dielectric loss in the GaN thin substrate is likely responsible for the noticeable insertion loss.

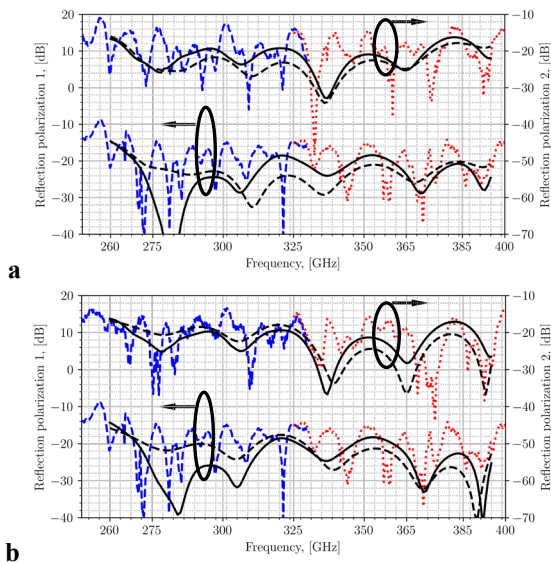


Figure 7. Measured and simulated S_{11} , S_{22} and S_{33} for polarization 1 & 2 in the OMT with the mounted chip Alternative 2. The measurements data in comparison with the simulations for two sets of material parameters, the legend the same as in Fig. 6.

Therefore possible improvements in the insertion loss could be expected by improving the processing and using superconducting material, e.g., Nb and NbTiN, for future OMTs used at cryogenic temperatures. Choosing other materials for the thin substrate, would improve the insertion loss component connected to the losses in dielectric.

5. Conclusion

In this paper, we presented the design and the performance of the novel OMT for mm and sub-mm wavelengths which combines the advantages of the turnstile configuration and features a hybrid approach where the polarization splitting part relies on a microfabricated thin substrate, while the rest of the OMT employs waveguide structures. The two fabricated and tested prototype OMTs show similar and solid performance providing better than 30 dB cross-pol suppression and matching at all ports better than -15 dB. Performance improvements are expected with refining the microfabricated part processing, operation at cryogenic temperatures with use of superconducting transmission lines. The OMT has demonstrated broad band performance with the 38,8% fractional bandwidth, RF band 260-385 GHz. With the microfabricated polarization splitting junction and relatively simple waveguide circuitry that also could be fabricated using photolithographically defined waveguide structures [13], the OMT has good chances scaling up to higher frequencies, probably up to 1.5 THz.

6. Acknowledgements

This work was supported by the Swedish National Research Council grant to the Onsala Space Observatory, the Swedish National facility for Radio Astronomy and by ESO ALMA Upgrade Studies Program under Agreement No. 108757/ESO/22/121629/AMA.

References

- [1] A. M. Bøifot, "Classification of ortho-mode transducers," *European Transactions on Telecommunications*, vol. 2, no. 5, pp. 503–510, 1991.
- [2] A. Navarrini, et. al., "A turnstile junction waveguide orthomode transducer for the 1 mm band," in *Proceedings of the 16th International Symposium on Space Terahertz Technology*, 2005, pp. 02–04.
- [3] P. Mauskopf, et. al., "Clover polarimetric detector - a novel design of an ortho-mode transducer at 150 and 225 GHz," *33rd International Conference on Infrared, Millimeter and Terahertz Waves*, 2008, pp. 1–2.
- [4] D. Henke, et. al., "Design of a 70–116 GHz W-band turnstile OMT," *2014 44th European Microwave Conference*, Rome, Italy, 2014, pp. 456–459, doi: 10.1109/EuMC.2014.6986469.
- [5] W. Shan, et. al., "Planar superconductor-insulator-superconductor mixer array receivers for wide field of view astronomical observation," in *Millimeter, Submillimeter, and Far-Infrared Detectors and Instrumentation for Astronomy IX*, SPIE, vol. 10708, 2018, pp. 125–139.
- [6] S. V. Koshevaya, et. al., "Amplification and nonlinear interaction of space charge waves of microwave band in heterogeneous gallium nitride films," *Radioelectronics and Communications Systems*, vol. 55, no. 7, pp. 289–298, 2012.
- [7] S. Krause, et. al., "Suspended GaN beams and thin substrates on Si as a platform for waveguide-based THz applications," *Journal of Micromechanics and Microengineering*, vol. 28, no. 10, p. 105 007, 2018.
- [8] J. Bonache, et. al., "Complementary split rings resonators (csrrs): Towards the miniaturization of microwave device design," *Journal of computational electronics*, vol. 5, pp. 193–197, 2006.
- [9] G. Reeves, et. al., "Obtaining the specific contact resistance from transmission line model measurements," *IEEE Electron Device Letters*, vol. 3, no. 5, pp. 111–113, 1982. doi:10.1109/EDL.1982.25502.
- [10] ZeGage™ 3D Optical Profiler, Zygo Corporation, Laurel Brook Road, Middlefield, CT 06455.
- [11] Klaassen, TO., et. al., "Optical Characterization of Absorbing Coatings for Sub-millimeter Radiation", in *Proceedings of the 26th International Conference on Infrared and Millimeter Waves*, 2001.
- [12] A. Navarrini, et. al. "Characterization techniques of millimeter-wave orthomode transducers (OMTs)," *Electronics*, vol. 10, no. 15, p. 1844, 2021.
- [13] V. Desmaris, et. al., "Terahertz components packaging using integrated waveguide technology," *IEEE MTT-S Int. Microwave Workshop Series on Millimeter Wave Integration Technologies*, 2011, pp. 81–84. doi: 10.1109/IMWS3.2011.6061893